Supporting information for

Ohmic heating synthesis and characterization of Zn(II), Cu(II) and Pd(II) complexes of heterocyclic-fused chlorins

Maria I. F. Moreira, José Almeida, Andreia Leite, Ana I. M. C. Lobo Ferreira,
Luís M. N. B. F. Santos, Ana M. G. Silva,* Maria Rangel

Contents

Selected literature strategies to obtain isoxazoline and isoxazolidine functionalized porphyrins or chlorins

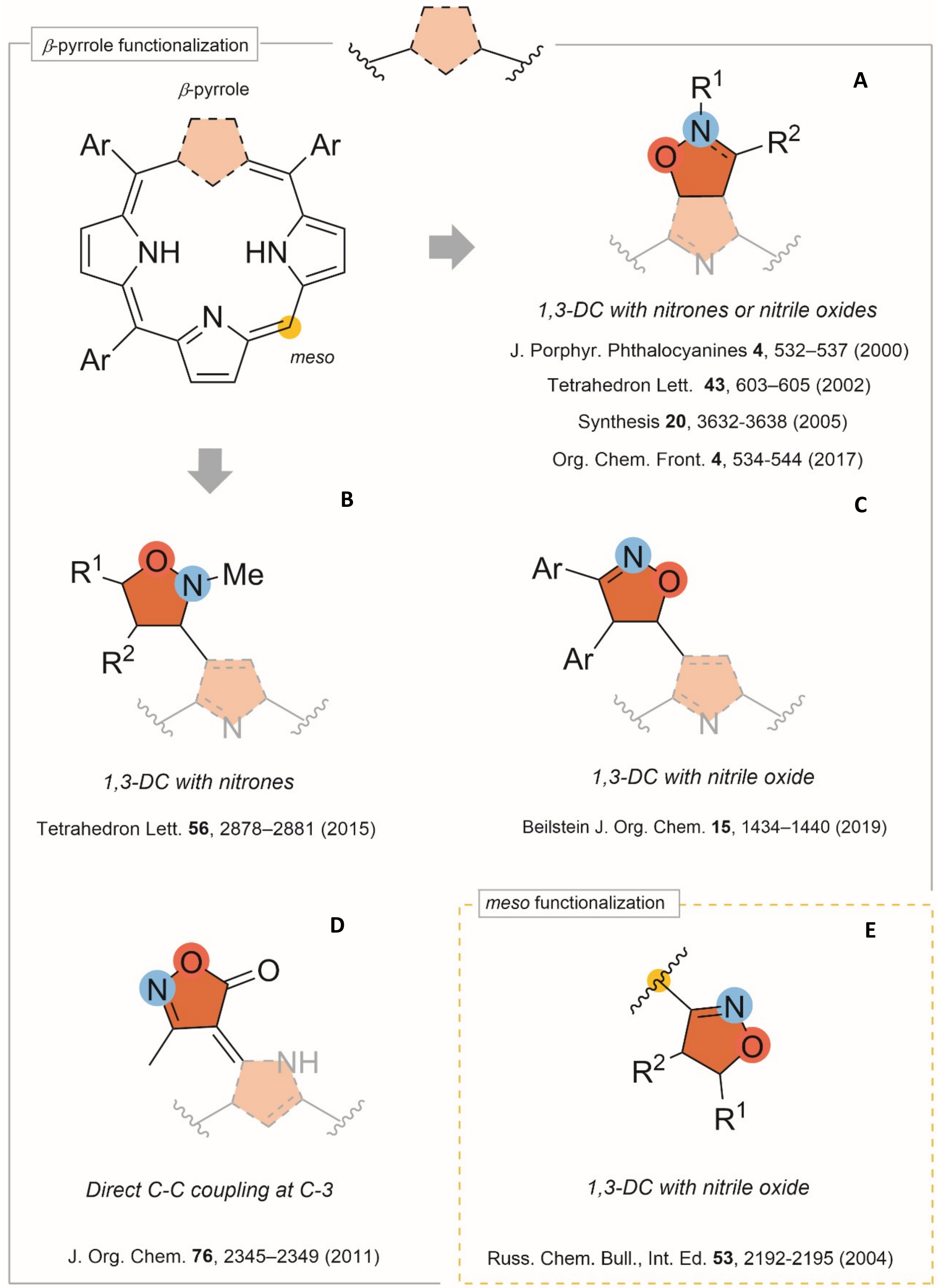

Scheme S1. Different strategies to synthesize isoxazoline and isoxazolidine functionalized porphyrins or chlorins: **A** - 1,3-dipolar cycloadditions (1,3-DC) of porphyrins acting as dipolarophiles with nitrones or nitrile oxides[1–4]; **B**, **C** - porphyrins acting as nitrones [5] or nitrile oxides precursors [6,7]; **D** - direct C-C coupling at the C-3 position of *N*-confused porphyrins[8] and **E** – *meso* substitution of porphyrin with isoxazoline.[7]

Names and abbreviations of metallochlorins

Table S1. Structure, name, molecular formula and exact mass of metallochlorins synthesised using ohmic heating (ΩH)

Structure	Name	Molecular formula	Exact Mass	Yield (%)
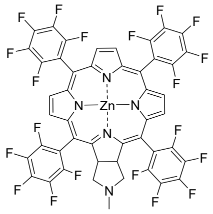	**Zn-1C**	$C_{47}H_{15}F_{20}N_5Zn$	1093.030	72
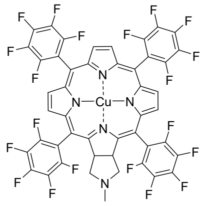	**Cu-1C**	$C_{47}H_{15}CuF_{20}N_5$	1092.030	70
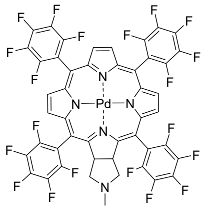	**Pd-1C**	$C_{47}H_{15}F_{20}N_5Pd$	1135.000	52
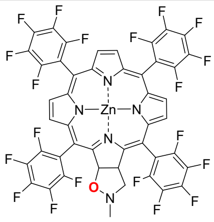	**Zn-2C**	$C_{46}H_{13}F_{20}N_5OZn$	1095.009	42
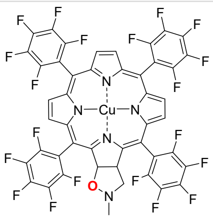	**Cu-2C**	$C_{46}H_{13}CuF_{20}N_5O$	1094.010	31
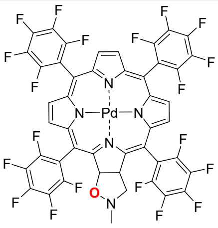	**Pd-2C**	$C_{46}H_{13}F_{20}N_5OPd$	1136.98	14

NMR spectra of Zn-1C

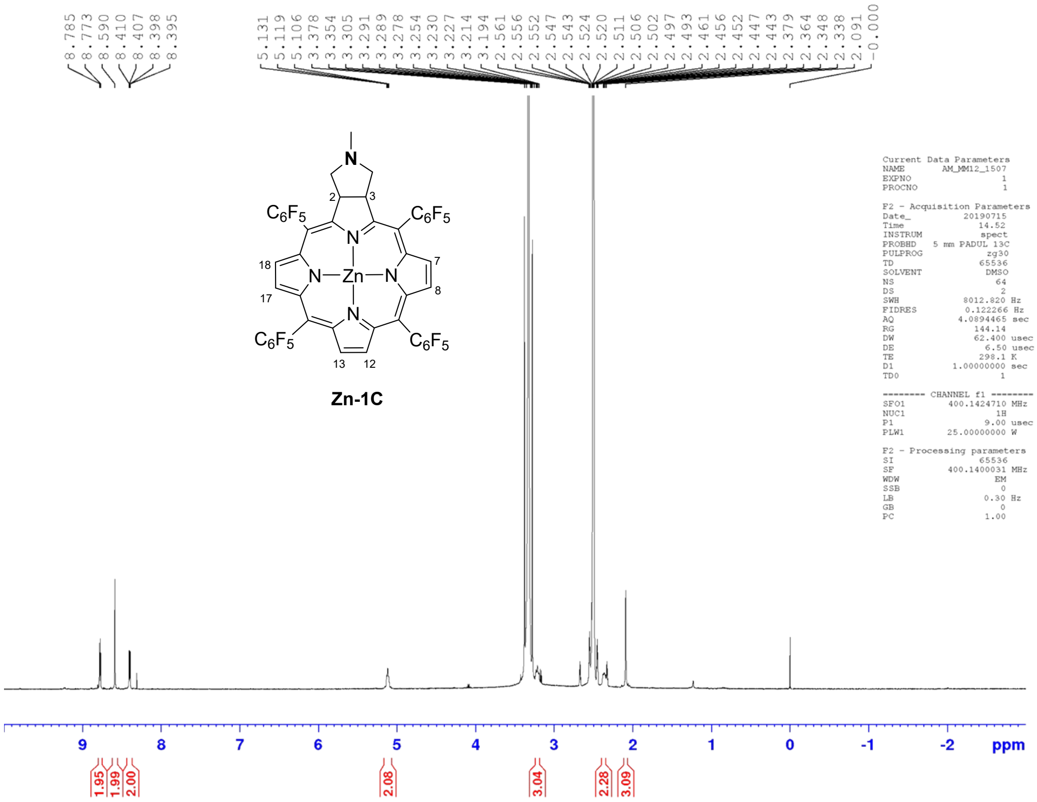

Figure S1. ^{1}H NMR spectrum (400.15 MHz, DMSO-d_6) of **Zn-1C**.

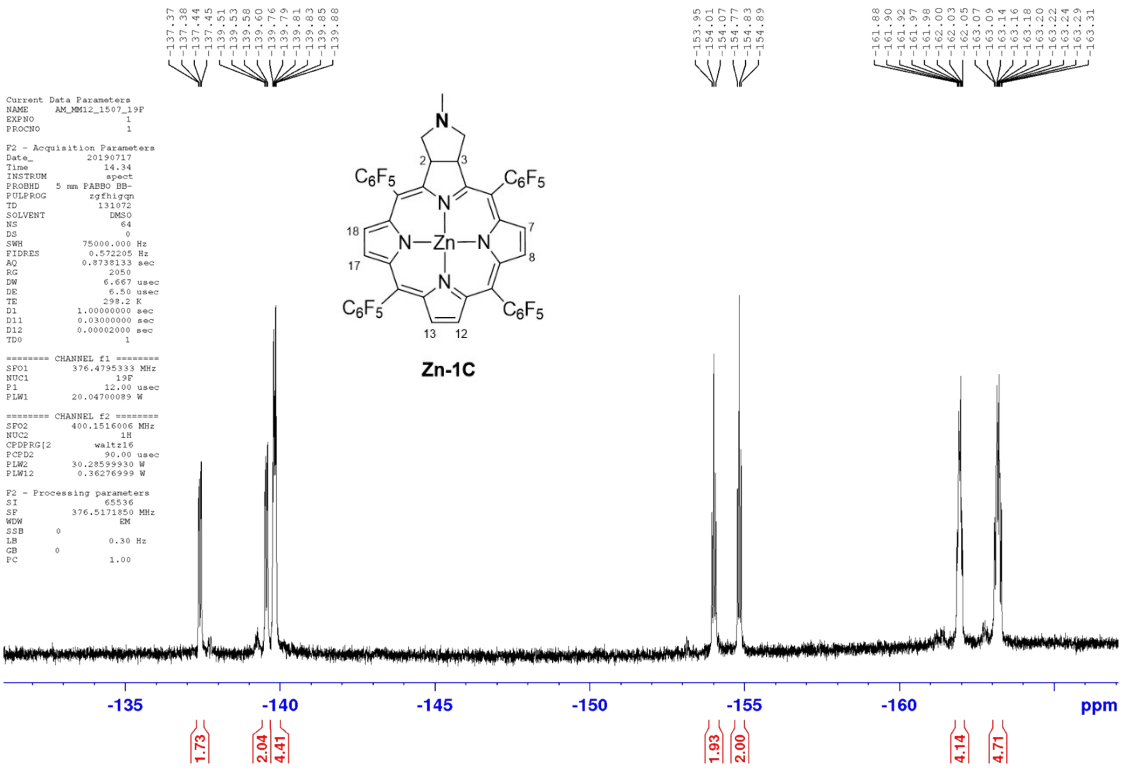

Figure S2. ^{19}F NMR spectrum (376.48 MHz, DMSO-d_6) of **Zn-1C**.

NMR spectra of Zn-2C

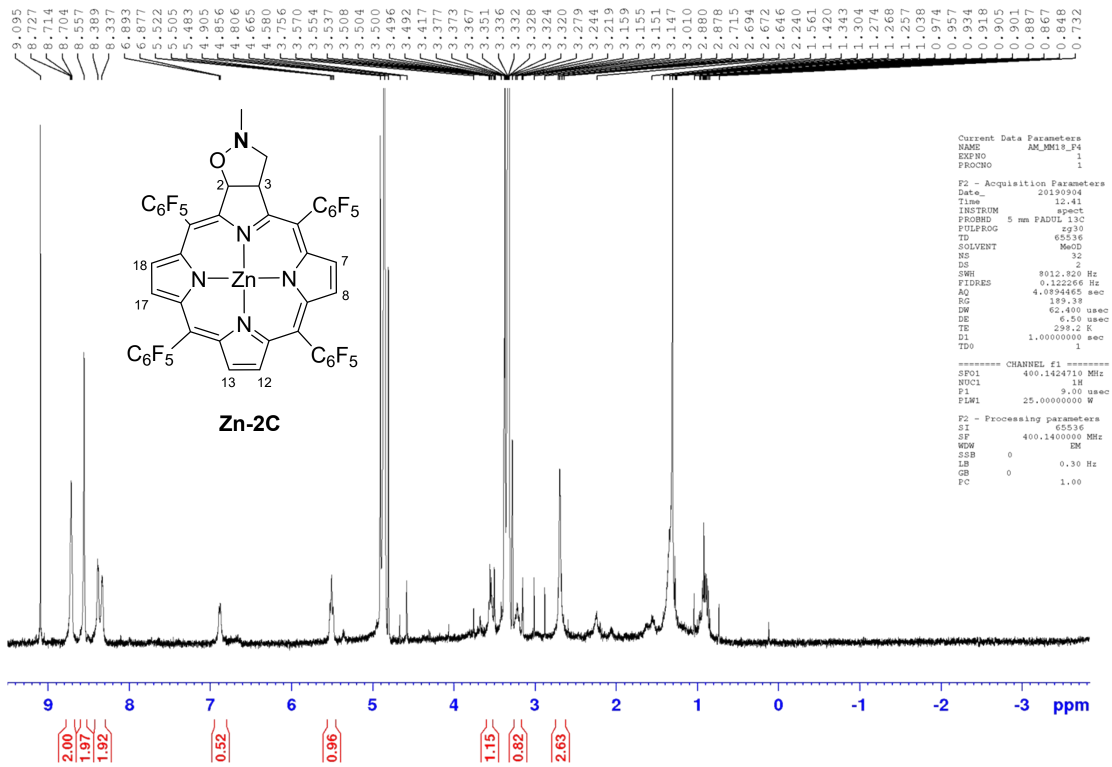

Figure S3. ^{1}H NMR spectrum (400.15 MHz, MeOD-d$_4$) of **Zn-2C**.

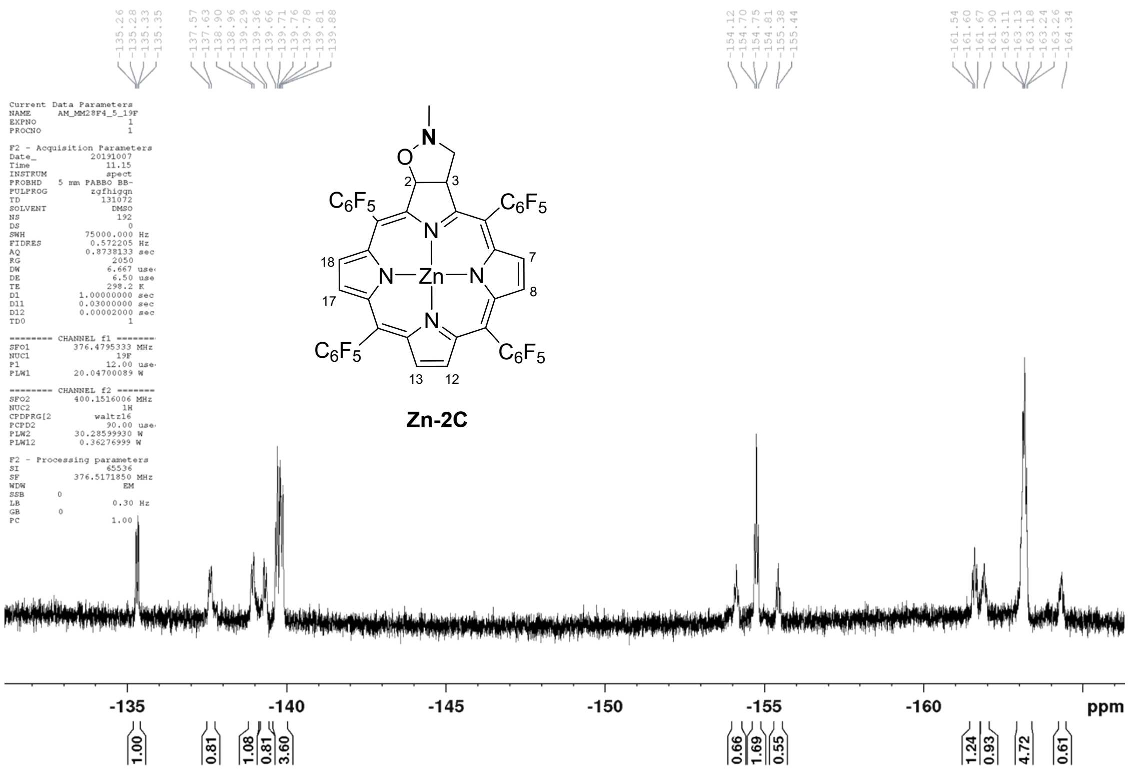

Figure S4. ^{19}F NMR spectrum (376.48 MHz, DMSO-d$_6$) of **Zn-2C**.

NMR spectra of Pd-1C

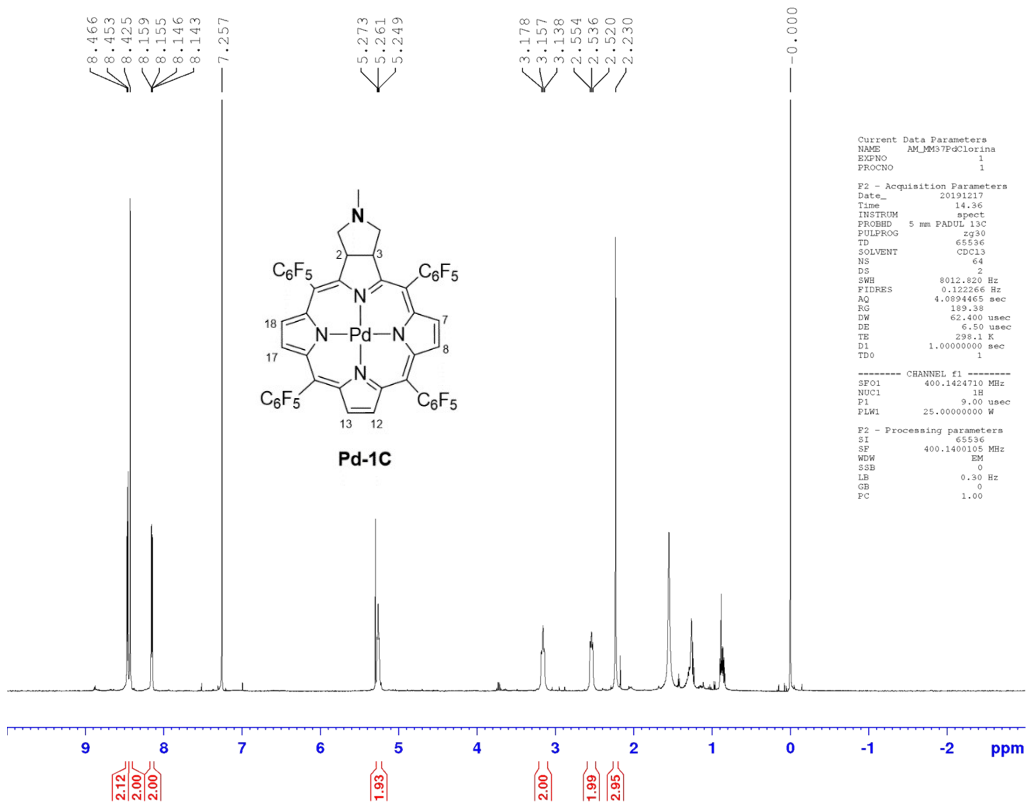

Figure S5. ^{1}H NMR spectrum (400.15 MHz, $CDCl_3$) of **Pd-1C**.

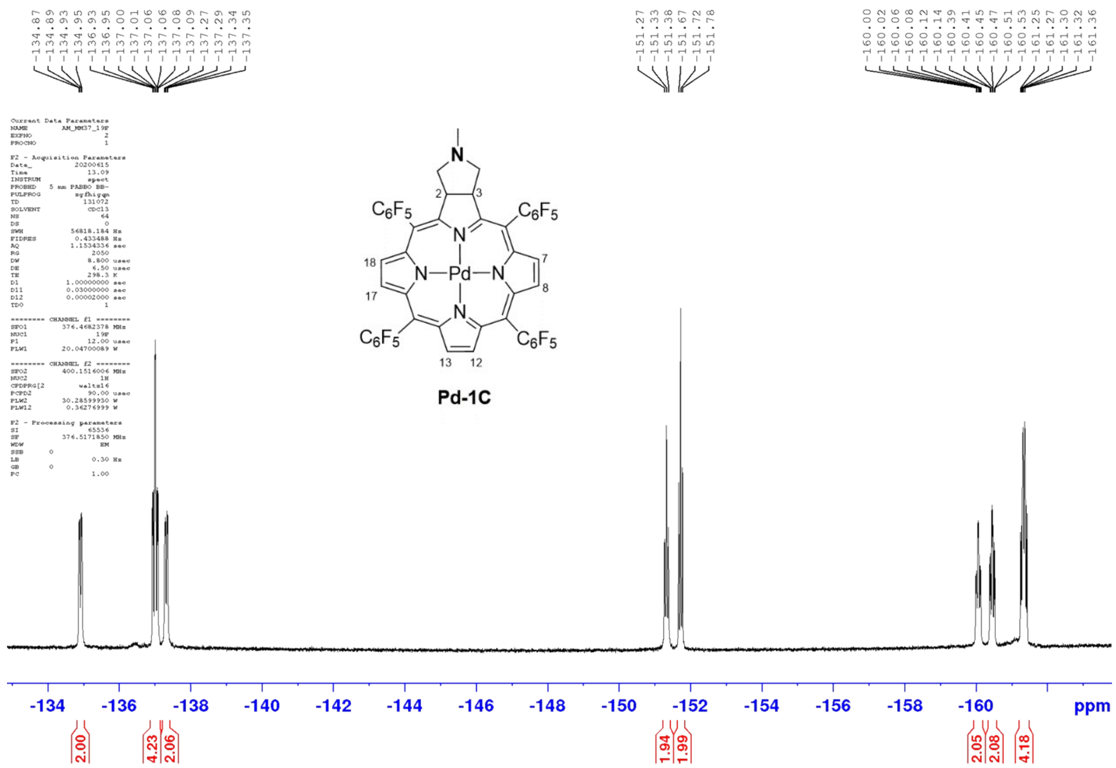

Figure S6. ^{19}F NMR spectrum (376.48 MHz, $CDCl_3$) of **Pd-1C**.

NMR spectra of Pd-2C

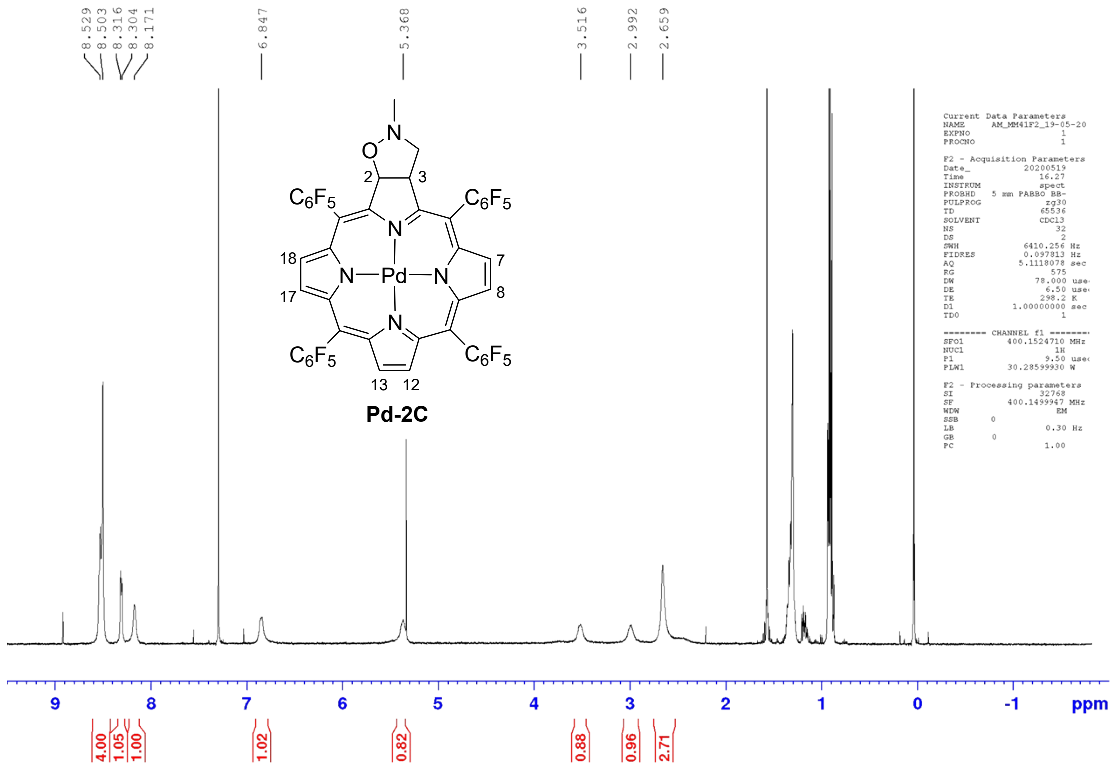

Figure S7. ^{1}H NMR spectrum (400.15 MHz, $CDCl_3$) of **Pd-2C**.

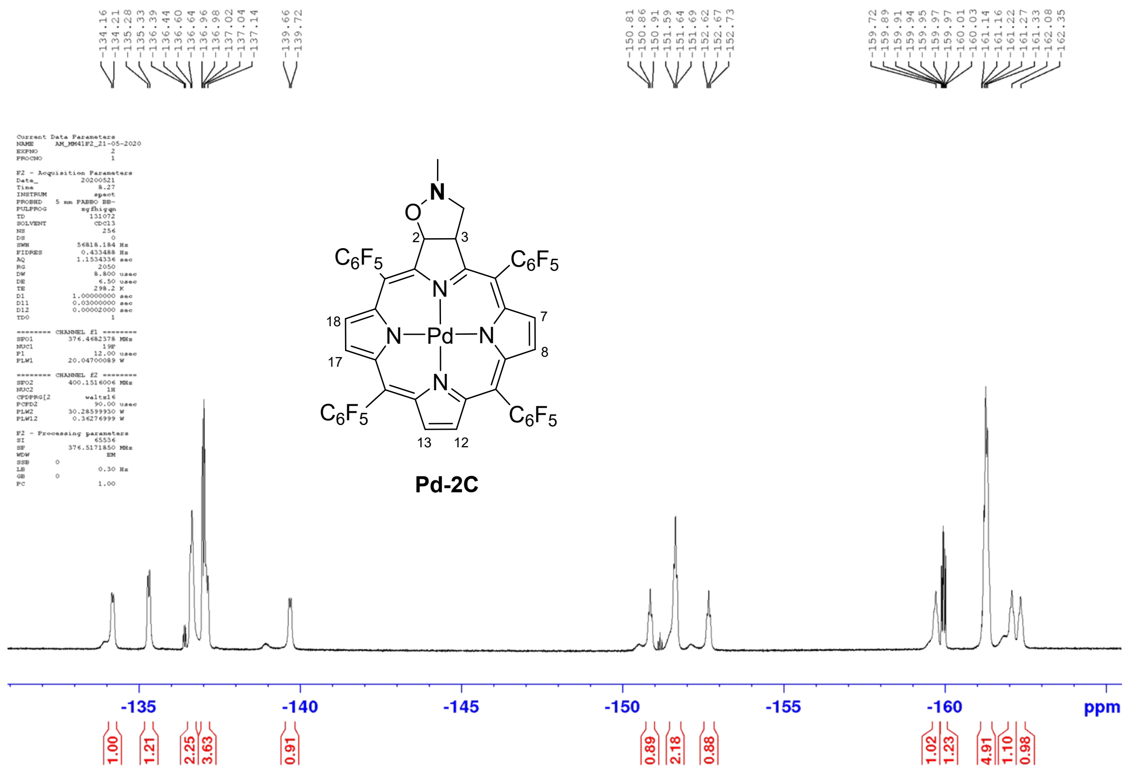

Figure S8. ^{19}F NMR spectrum (376.48 MHz, $CDCl_3$) of **Pd-2C**.

MS spectra of metallochlorins

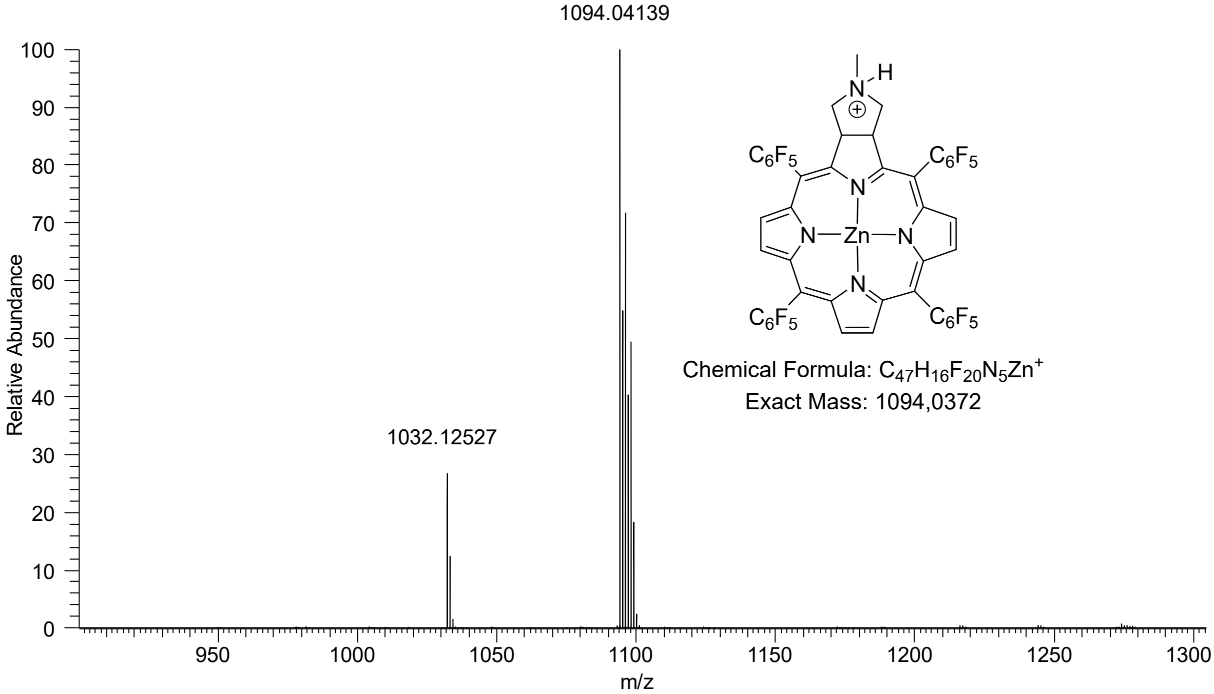

Figure S9. HRMS (ESI) spectrum of **Zn-1C**.

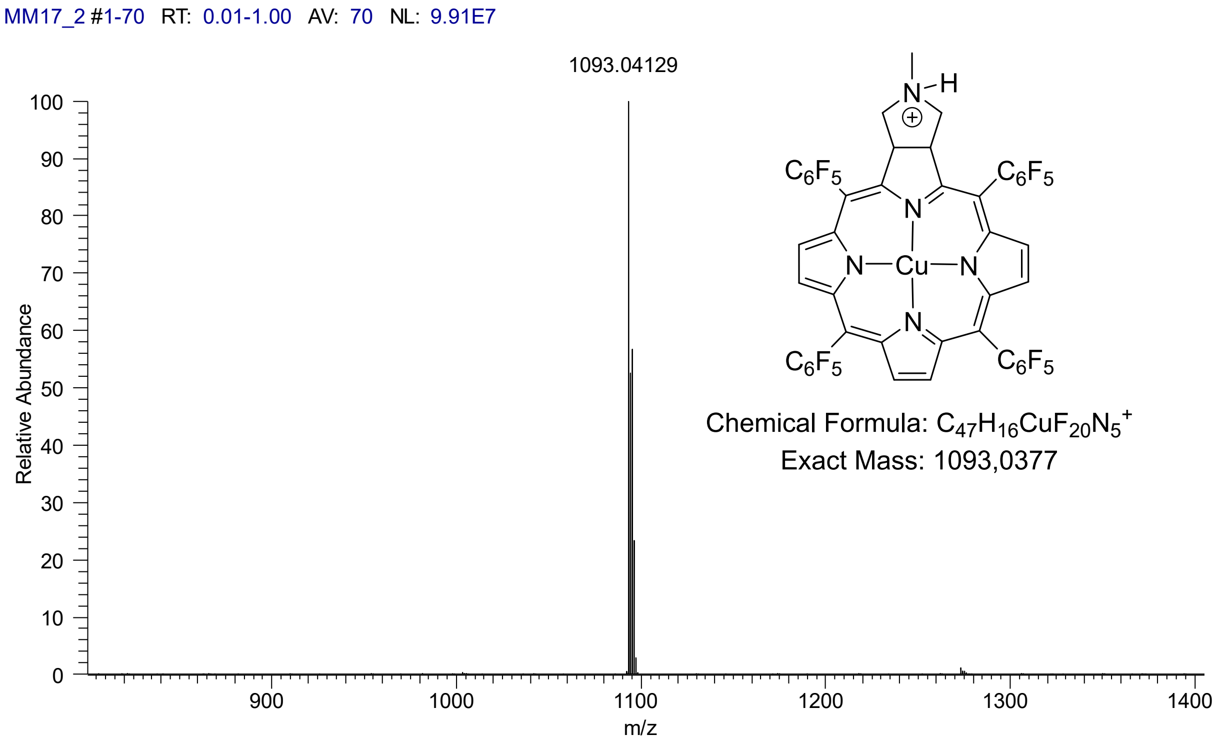

Figure S10. HRMS (ESI) spectrum of **Cu-1C**.

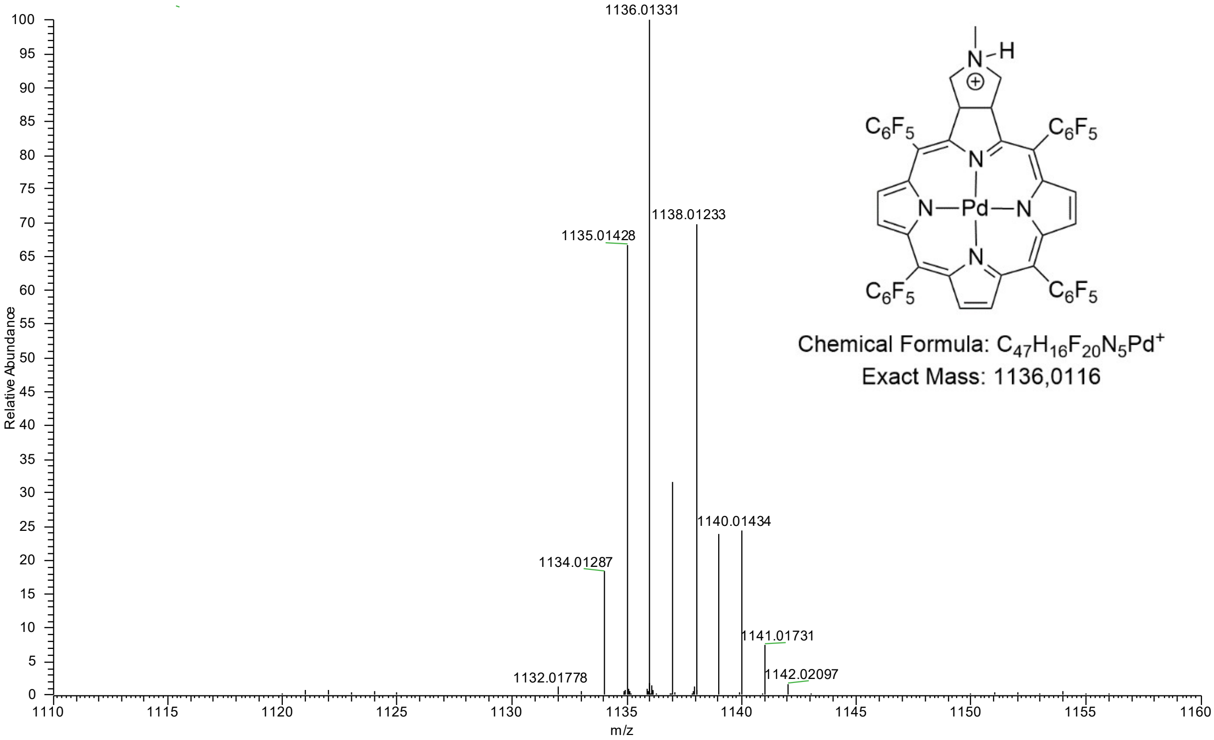

Figure S11. HRMS (ESI) spectrum of **Pd-1C**.

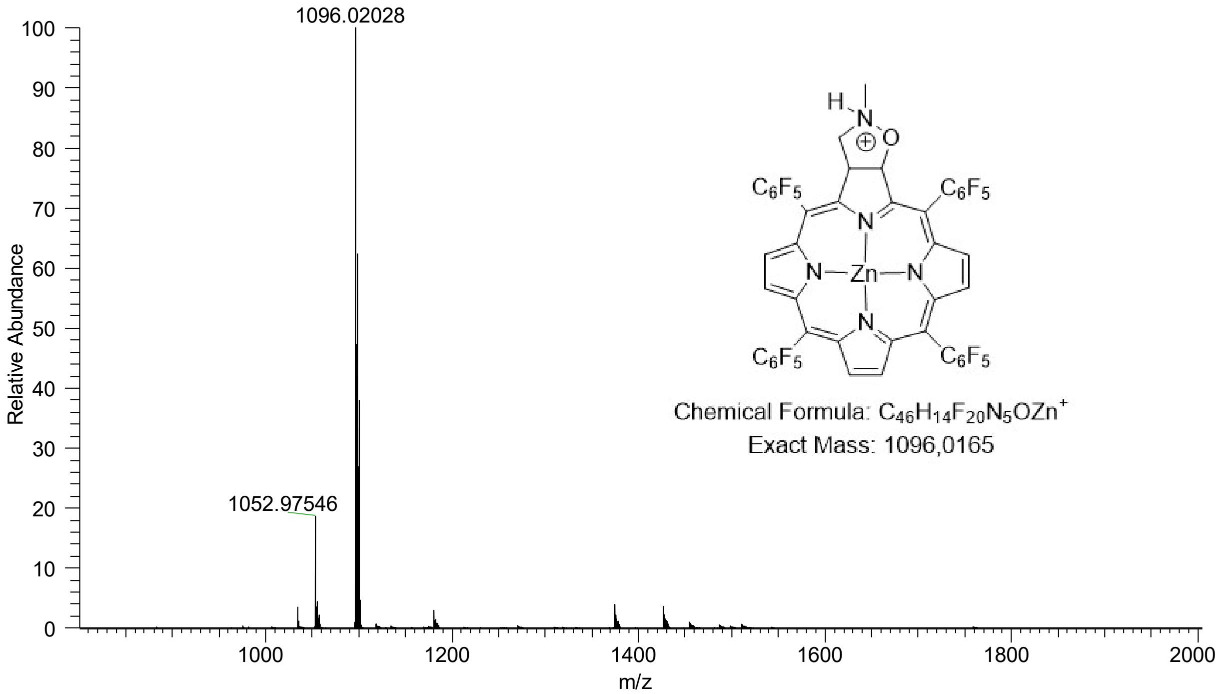

Figure S12. HRMS (ESI) spectrum of **Zn-2C**.

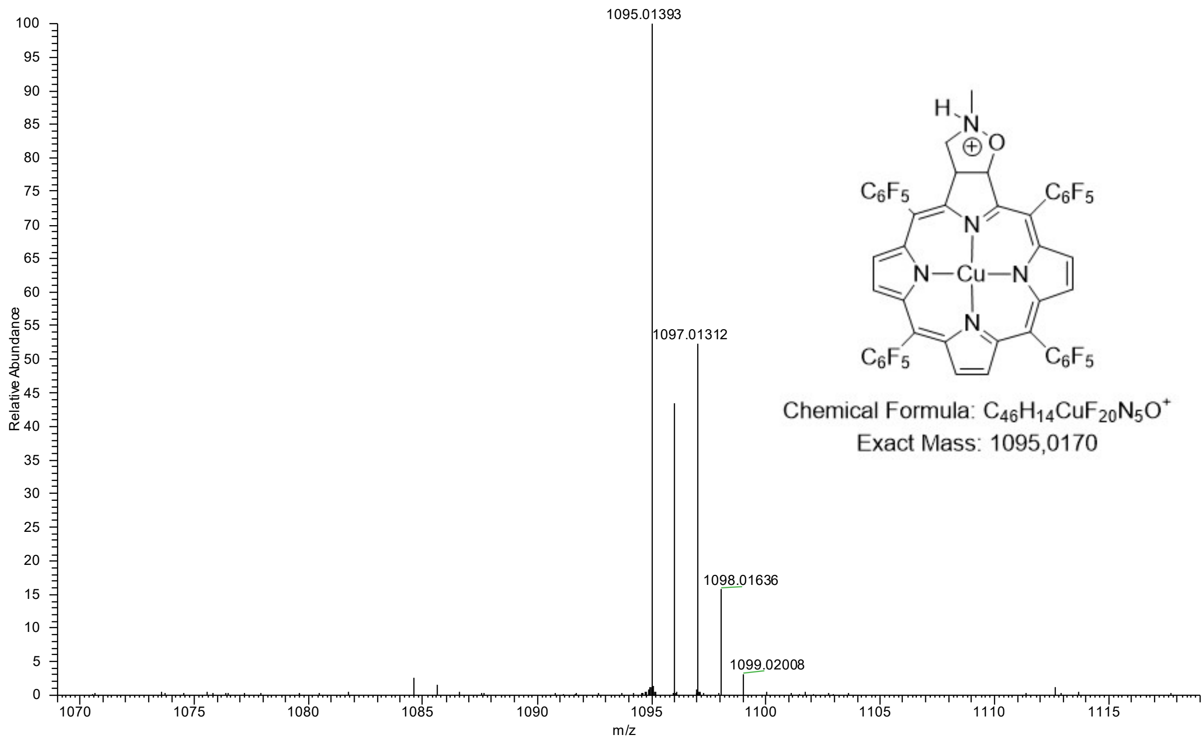

Figure S13. HRMS (ESI) spectrum of **Cu-2C**.

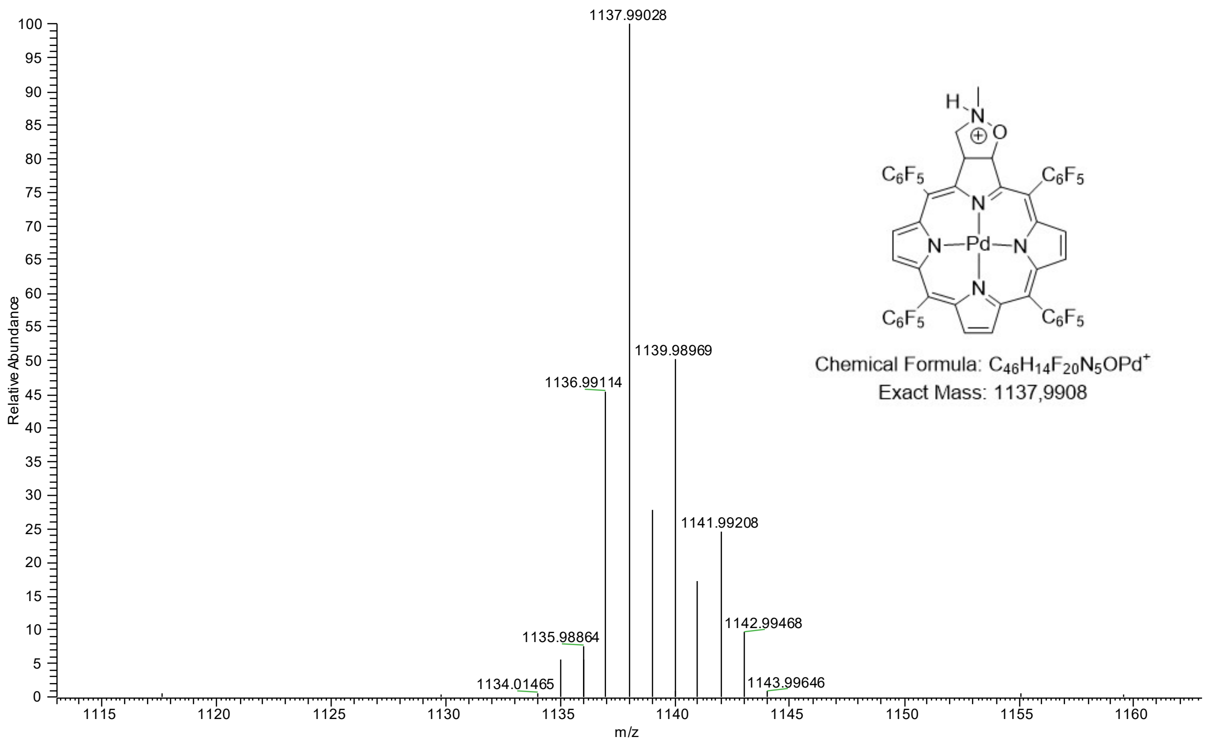

Figure S14. HRMS (ESI) spectrum of **Pd-2C**.

Ohmic heating reactor

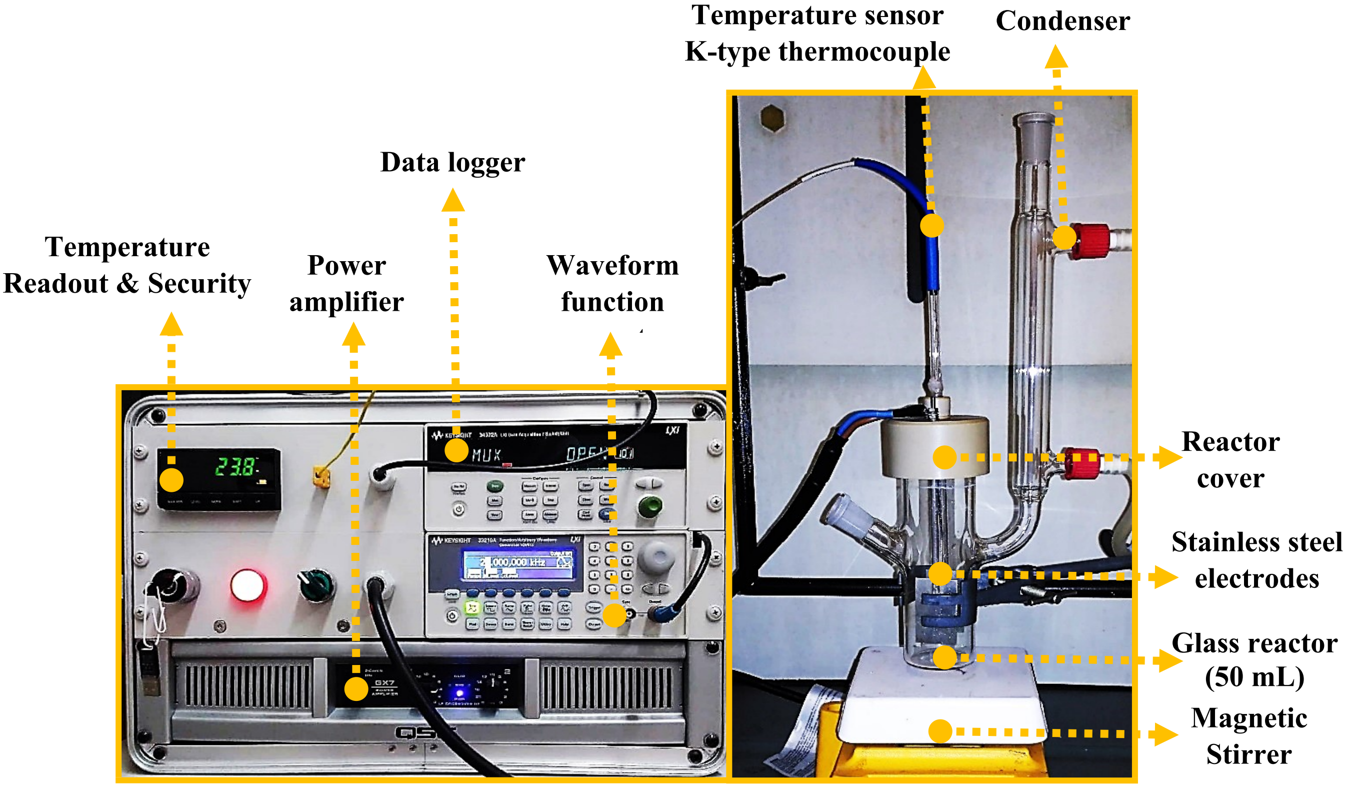

Figure S15: ΩH reactor (Portuguese Patent No. 105908, 2011-09-27). The reactor description: VAC power supply; 33210A waveform function generator; heating reactor cell (50 mL glass vessel) containing one pair of stainless steel (316) rectangular electrodes (40×25×1 mm length/width/thickness) located at a fixed distance (23 mm) and in contact with the reaction medium; temperature sensor (K-type thermocouple); 34970A data logger system; PC computer; data acquisition and control software package.

Ohmic heating reactions (Temperature, Power, AC Current Intensity, AC Voltage and Impedance versus reaction heating time)

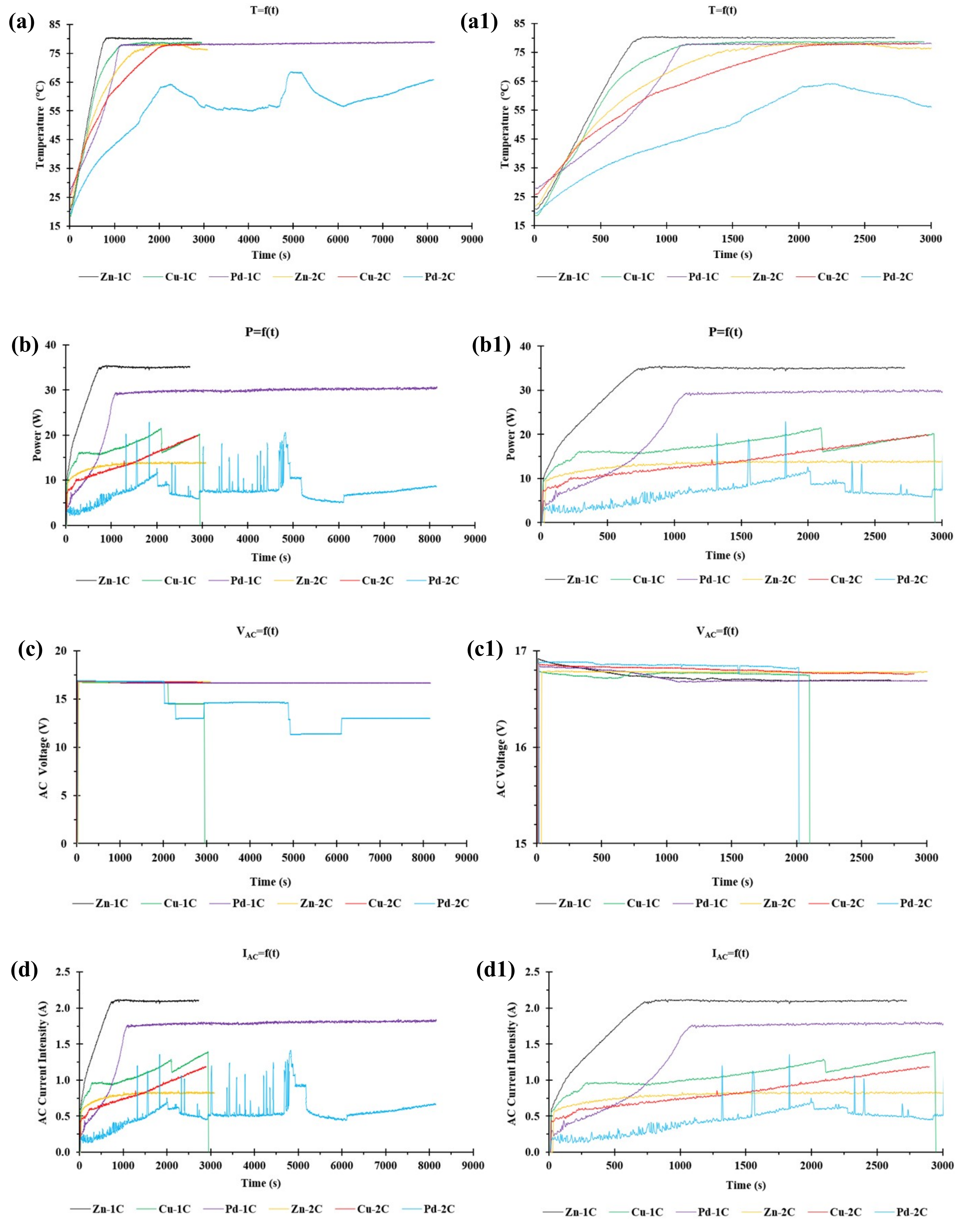

Figure S16. Graphics exhibiting the monitoring of the ohmic heating reactions of **Zn-1C**, **Cu-1C**, **Pd-1C**, **Zn-2C**, **Cu-2C** and **Pd-2C**. (**a**) Temperature versus reaction heating time; **(a1)** a close-up of figure (**a**); (**b**) Power versus reaction heating time; **(b1)** A close-up of figure (**b**); (**c**) AC Voltage versus reaction heating time; **(c1)** a close-up of figure (**c**). (**d**) AC Current Intensity versus reaction heating time; **(d1)** a close-up of figure (**d**).

Table S2: Results obtained in the ΩH metallations using different Zn(II), Cu(II) and Pd(II) salts. Reaction scope and yields. Lines in blue represent the most favourable conditions found for the synthesis of the desired metallochlorins

Metallochlorin	Metal Salt	Metal Salt (g)	NaCl (g)	CH_3COONa (g)	Temperature (ºC)	Time (min)	AC Voltage (V)	AC Current Intensity (A)	Impedance (Ω)	Power (W)	Yield (%)
Zn-1C	$ZnSO_4$	1.50	0.500	-	78.1	45	16.8	1.62	10.3	27.3	72
	$Zn(OAc)_2$	1.50	0.500	-	80.1	45	16.7	2.11	7.92	35.2	76
	$ZnCl_2$	1.50	-	-	71.6	45	16.9	0.810	20.8	13.7	72
Cu-1C	**$CuCl_2$**	1.50	-	-	78.6	45	14.5	1.36	10.7	19.8	70
Pd-1C	$PdCl_2$	1.00	0.500	-	77.2	135	16.8	1.34	12.5	22.5	2
	$Pd(OAc)_2$	1.00	-	2.00	78.8	135	16.7	1.82	9.17	30.4	52
Zn-2C	**$ZnCl_2$**	1.50	-	-	76.5	45	16.8	0.818	20.2	13.9	42
Cu-2C	**$CuCl_2$**	1.00	-	-	78.2	45	16.8	1.18	14.1	19.5	31
Pd-2C	**$Pd(OAc)_2$**	0.50	-	2.00	65.9	135	13.0	0.663	19.6	8.63	14

EPR spectra

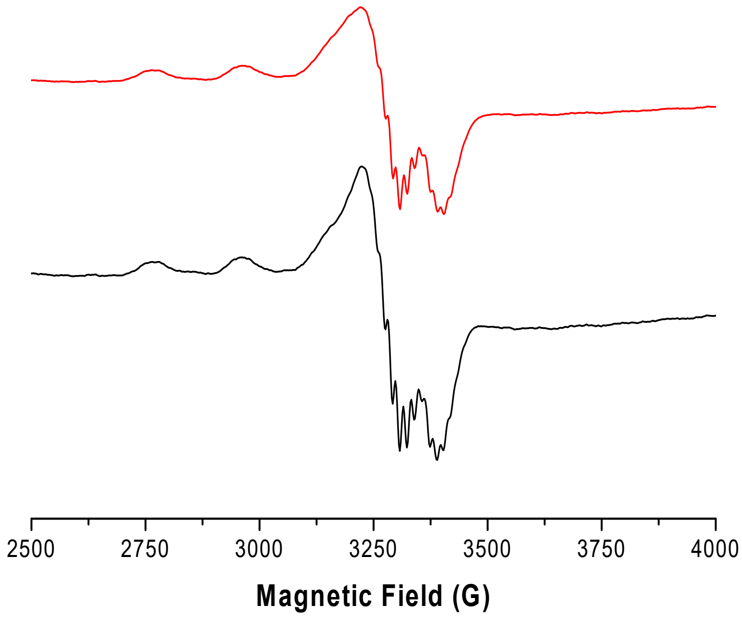

Figure S17: EPR spectrum of **Cu-1C** (black line) and EPR spectrum of **Cu-1C** obtained by computer simulation (red line).

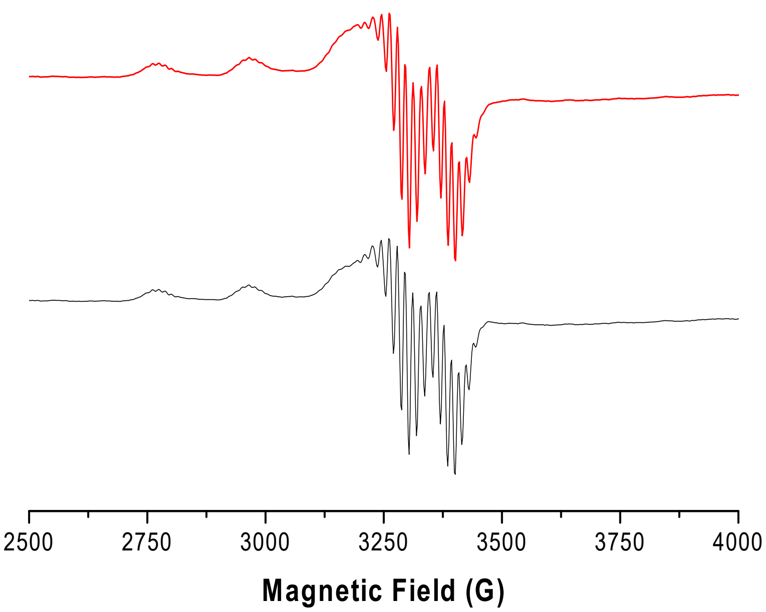

Figure S18: EPR spectrum of **Cu-2C** (black line) and EPR spectrum of **Cu-2C** obtained by computer simulation (red line).

Table S3: Spin-Hamiltonian parameters for **Cu-1C** and **Cu-2C**

	g_x	g_y	g_z		**A_x (Gauss)**	**A_y (Gauss)**	**A_z (Gauss)**
Cu-1C	2.064	2.060	2.198	Cu	36	36	208
				$^{14}N_{1,3}$	28	15	15
				$^{14}N_{2,4}$	15	15	28
Cu-2C	2.066	2.066	2.188	Cu	36	36	212
				$^{14}N_{1,3}$	20	15	15
				$^{14}N_{2,4}$	15	15	20

Photophysical studies

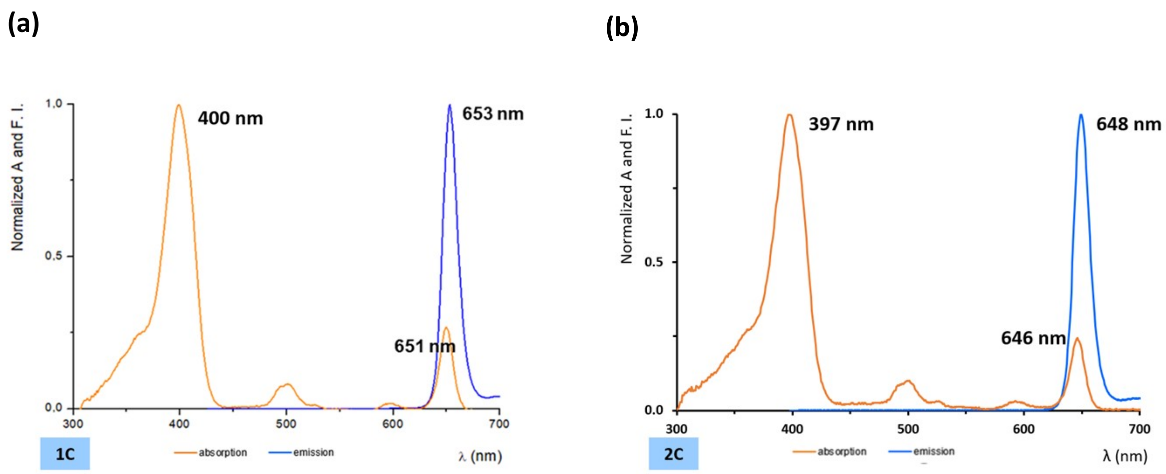

Figure S19: Absorption and emission spectra of **(a)** chlorin **1C** and **(b)** chlorin **2C** in methanol. Emission spectra were recorded using the following excitation wavelengths: λ_{exc} = 400 nm for **1C** and λ_{exc} = 397 nm for **2C**.

Table S4. Absorption and emission spectra data for synthesized metallochlorins in methanol.

	Absorption λ_{max}[nm] (ε_{max} [mol^{-1} dm^3cm^{-1}])				**Emission**	
Compound	**Soret Band**	**Q Bands**			**λ_{max}[nm]**	**Φ_F (%)**
Zn-1C	413 (262×10^3)	514 (5.6×10^3)	581 (7.5×10^3)	618 (49×10^3)	621	5.9
Cu-1C	408 (172×10^3)	503 (5.1×10^3)	571 (7.2×10^3)	615 (39×10^3)	N.O.[(a)]	0.2

Pd-1C	400 (184 × 10^3)	488 (8.8 × 10^3)	557 (12 × 10^3)	599 (74 × 10^3)	654	0.9
Zn-2C	412 (314 × 10^3)	516 (6.5 × 10^3)	586 (7.5 × 10^3)	617 (53 × 10^3)	647	5.6
Cu-2C	407 (235 × 10^3)	506 (6.2 × 10^3)	570 (8.7 × 10^3)	610 (47 × 10^3)	N.O.[(a)]	0.4
Pd-2C	399 (206 × 10^3)	487 (9.8 × 10^3)	554 (13 × 10^3)	595 (77 × 10^3)	N.O.[(a)]	0.5

[(a)] The emission spectrum was not observable, or too low in intensity to be observed.

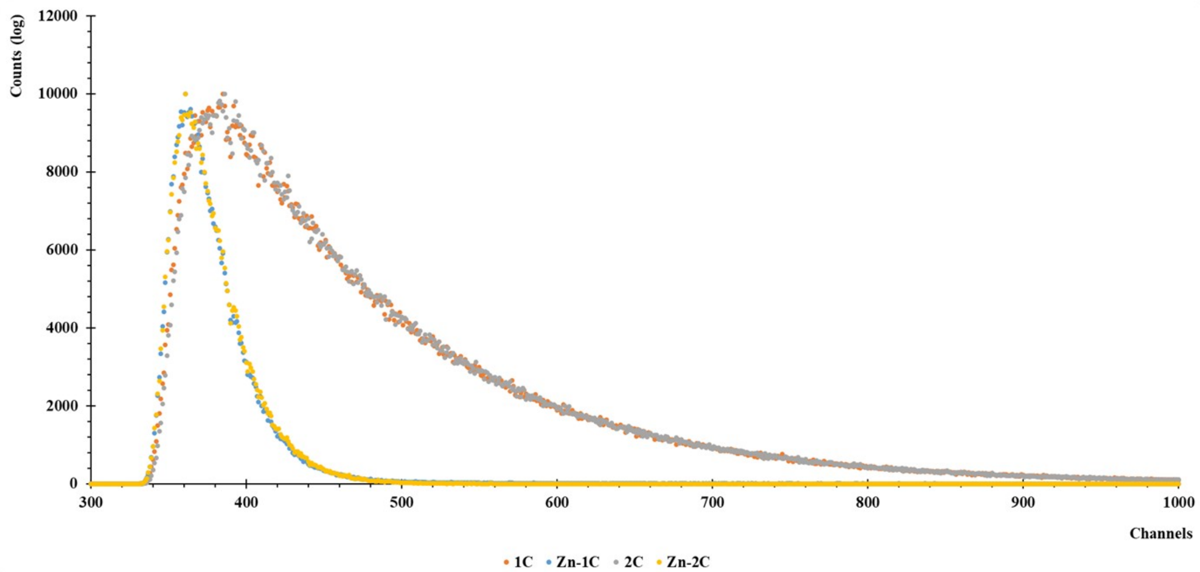

Figure S20: Experimental data obtained from time-resolved fluorescence spectroscopy, at the maximum emission wavelength of **1C**, **Zn-1C**, **2C**, **Zn-2C**. The excitation-emission process is repeated many times (usually to 10,000 counts in the peak channel), which will build up a histogram of number of events (counts) versus channels. Fewer channels will also reflect in more background noise.

DSC and TG measurements

Thermal stability was evaluated by thermogravimetric analysis (TGA) using a NETZSCH model TG 209 F1 Iris thermomicrobalance. The TGA experiments were performed in inert atmosphere using nitrogen (99.999%, protective gas: 20 mL·min^{-1}, purge gas: 20 mL·min^{-1}). The sample was placed in aluminum crucibles (NETZSCH, ø = 6 mm, volumetric capacity of 25 μL) and was heated from 303 K to 743 K at a scan rate of 5 K·min^{-1}.

The thermal behavior of the metallochlorins was also explored in the temperature range of 323 K to 643 K using a differential scanning calorimeter DSC (NETZCH, model DSC 200 F3 Maia): scanning rate, β = 5 K·min^{-1}, T_i = 303 K (30 °C), T_f = 643 K (370 °C) for the pyrrolidine-fused metallochlorins (**1C**; **Zn-1C**; **Cu-1C**; **Pd-1C**) and T_i = 303 K (30 °C), T_f = 573 K (300 °C) for the isoxazolidine-fused metallochlorins (**2C**; **Zn-2C**; **Cu-2C**; **Pd-2C**). DSC experiments were done using hermetically sealed aluminum crucibles (volumetric capacity of 50 μL) and a constant flow of nitrogen (99.999%, 50 mL·min^{-1}).

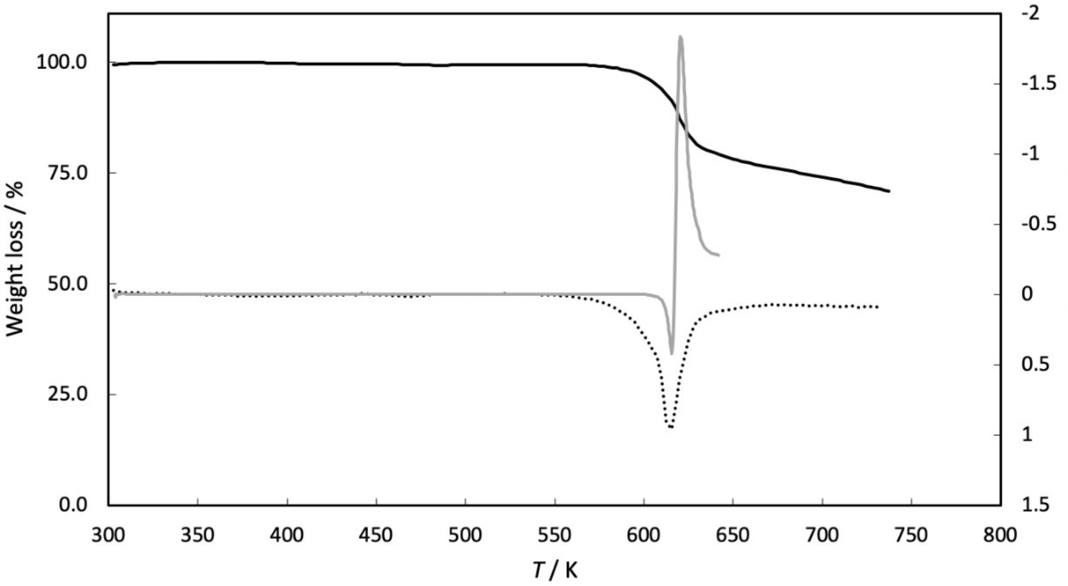

Figure S21. Mass loss and heat flux as function of temperature for the **1C**. TG [–] and DTG (1st derivative), [····] experiment: m_i = 5.978 mg, DSC [–] experiment: m_i = 11.3741 mg.

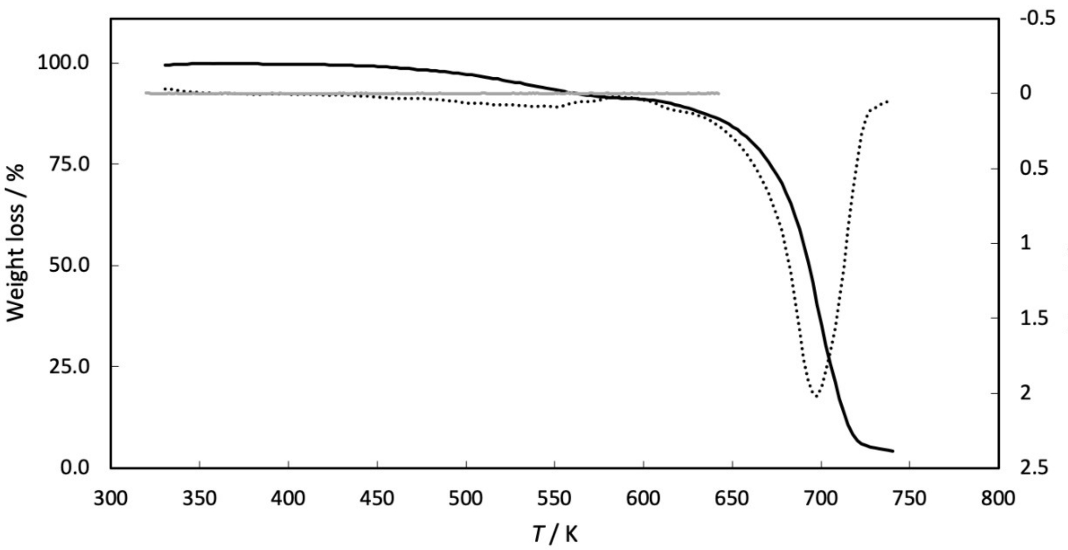

Figure S22. Mass loss and heat flux as function of temperature for the **Zn-1C**. TG [–] and DTG (1st derivative), [····] experiment: m_i = 0.343 mg, DSC [–] experiment: m_i = 1.1204 mg.

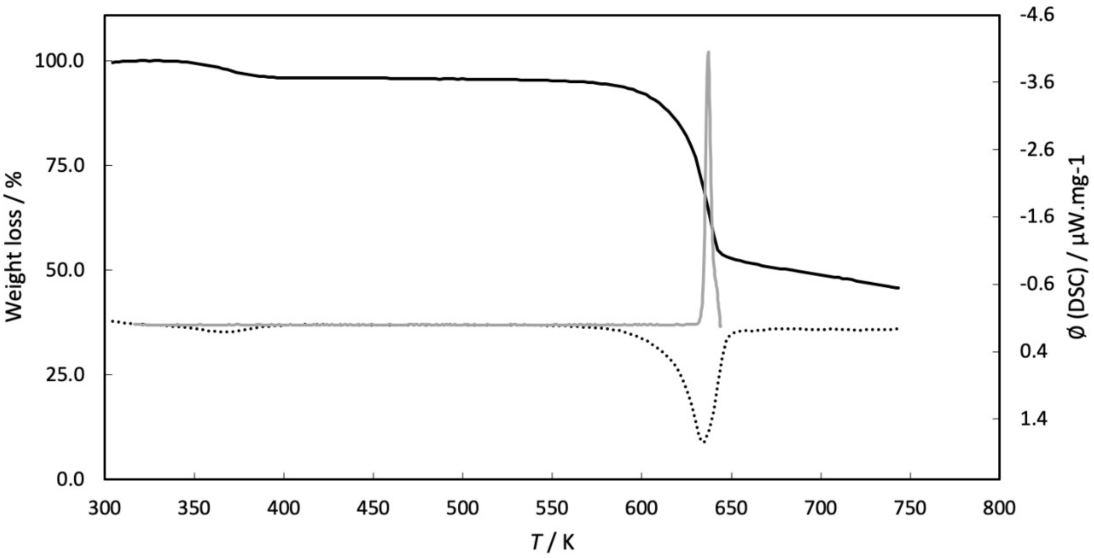

Figure S23. Mass loss and heat flux as function of temperature for the **Cu-1C**. TG [–] and DTG (1st derivative), [····] experiment: m_i = 2.088 mg, DSC [–] experiment: m_i = 4.6243 mg.

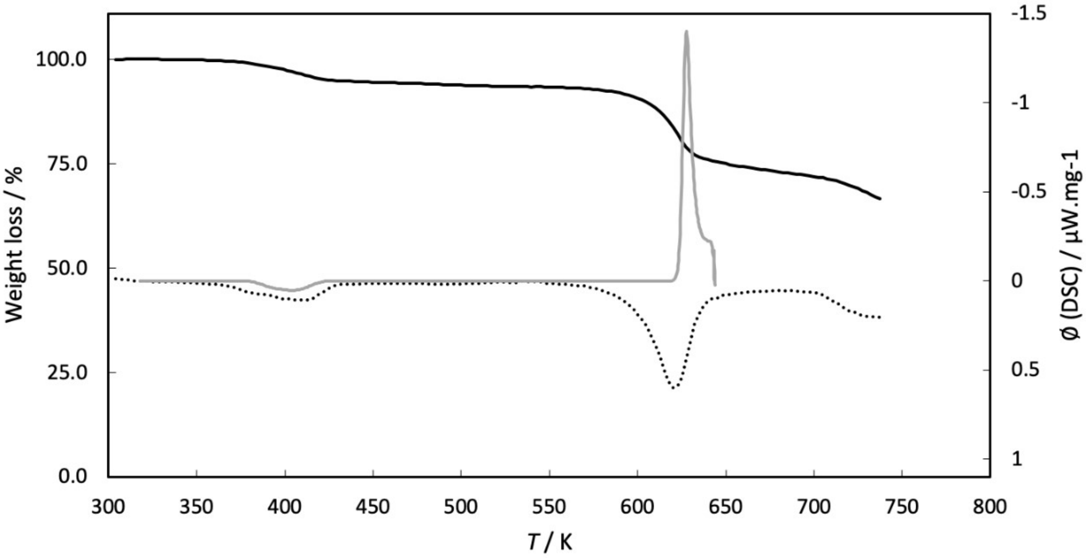

Figure S24. Mass loss and heat flux as function of temperature for the **Pd-1C**. TG [–] and DTG (1st derivative), [····] experiment: m_i = 3.668 mg, DSC [–] experiment: m_i = 6.6071 mg.

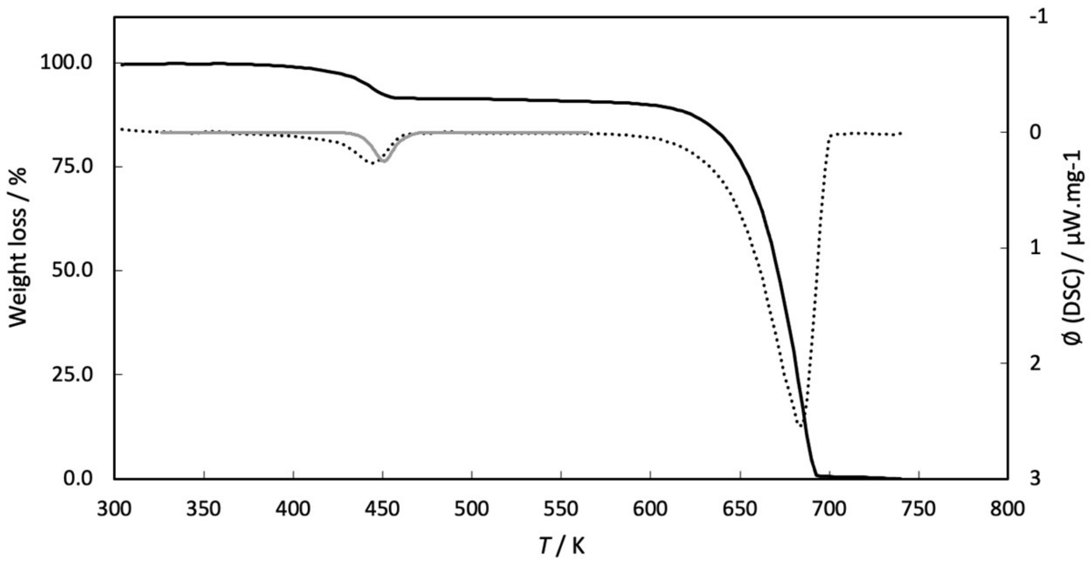

Figure S25. Mass loss and heat flux as function of temperature for the **2C**. TG [–] and DTG (1st derivative), [····] experiment: m_i = 2.922 mg, DSC [–] experiment: m_i = 3.2952 mg.

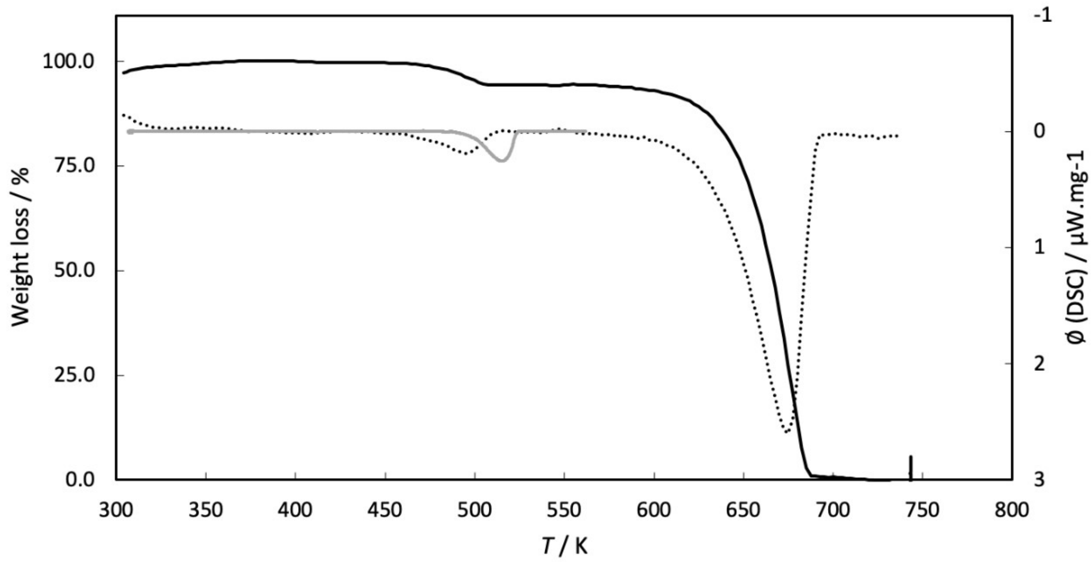

Figure S26. Mass loss and heat flux as function of temperature for the **Zn-2C**. TG [–] and DTG (1st derivative), [····] experiment: m_i = 1.201 mg, DSC [–] experiment: m_i = 2.2944 mg.

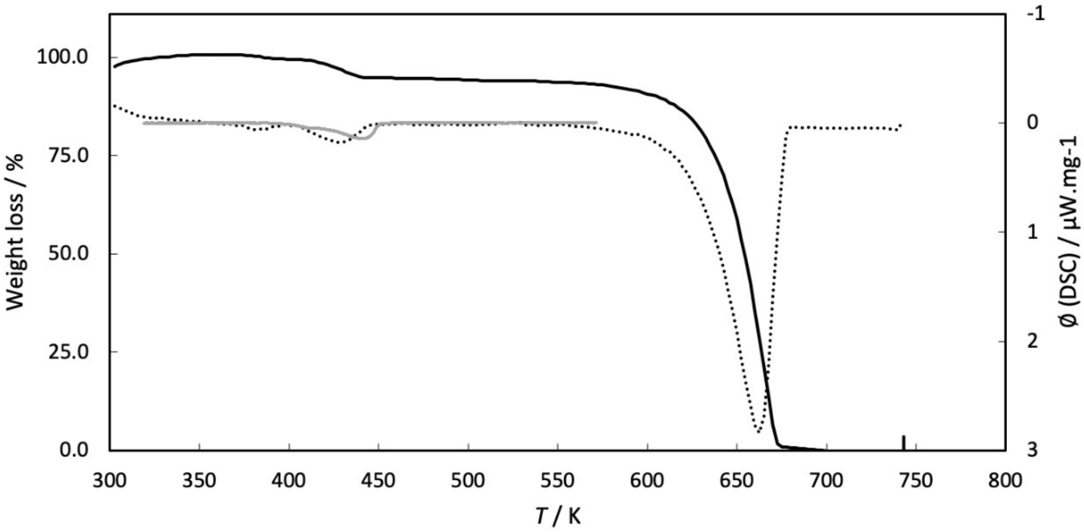

Figure S27. Mass loss and heat flux as function of temperature for the **Cu-2C**. TG [–] and DTG (1st derivative), [····] experiment: m_i = 1.088 mg, DSC [–] experiment: m_i = 3.7807 mg.

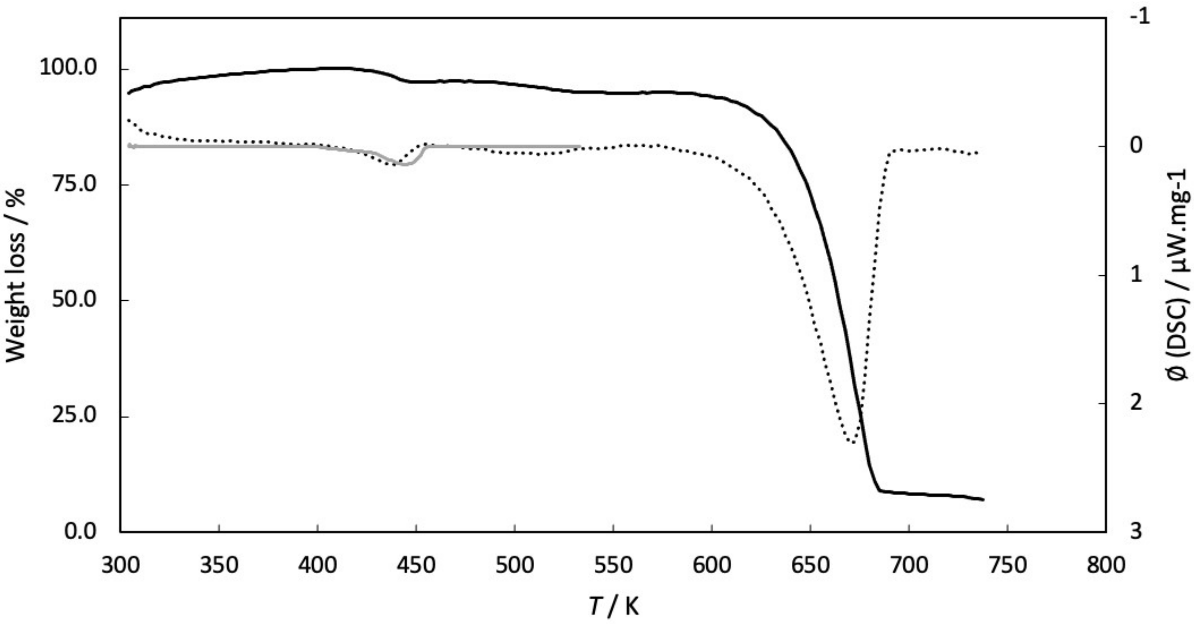

Figure S28. Mass loss and heat flux as function of temperature for the **Pd-2C**. TG [–] and DTG (1st derivative), [····] experiment: m_i = 0.957 mg, DSC [–] experiment: m_i = 3.3299 mg.

References

1 L. Xingang, F. Yaqing, H. Xiaofen and L. Xianggao, *Synthesis*, 2005, **2005**, 3632–3638.

2 J. Almeida, A. Aguiar, A. Leite, A. M. N. Silva, L. Cunha-Silva, B. de Castro, M. Rangel, G. Barone, A. C. Tomé and A. M. G. Silva, *Organic Chemistry Frontiers*, 2017, **4**, 534–544.

3 J. A. S. Cavaleiro, M. G. P. M. Neves, A. C. Tome, A. M. S. Silva, M. A. F. Faustino, P. S. Lacerda and A. M. G. Silva, *Journal of Heterocyclic Chemistry*, 2000, **37**, 527–534.

4 A. M. G. Silva, A. C. Tomé, M. G. P. M. S. Neves, A. M. S. Silva, J. A. S. Cavaleiro, D. Perrone and A. Dondoni, *Tetrahedron Letters*, 2002, **43**, 603–605.

5 A. F. F. da Silva, J. F. B. Barata, A. M. G. Silva, M. G. P. M. S. Neves, A. C. Tomé, A. M. S. Silva and J. A. S. Cavaleiro, *Tetrahedron Letters*, 2015, **56**, 2878–2881.

6 X. Liu, X. Ma and Y. Feng, *Beilstein Journal of Organic Chemistry*, 2019, **15**, 1434–1440.

7 Yu. V Morozova, Z. A. Starikova, B. I. Maksimov, D. V Yashunskii and G. V Ponomarev, *Russian Chemical Bulletin*, 2004, **53**, 2192–2195.

8 X. Li, B. Liu, P. Yi, R. Yi, X. Yu and P. J. Chmielewski, *The Journal of Organic Chemistry*, 2011, **76**, 2345–2349.

9 Yu. V. Morozova, Z. A. Starikova, B. I. Maksimov, D. V. Yashunskii and G. V. Ponomarev, *Russian Chemical Bulletin*, 2004, **53**, 2192–2195.